Supporting Information

Interfacial Chemistry and Ion Transfer Mechanism for Tailored Poly(thioether) Enabled Hybrid Solid Polymer Electrolyte with Electrochemical Properties in All-Solid-State Lithium-Sulfur Batteries

Yuhan Li,[a,1] Kai Xi,[b,1] Mingbo Ma,[b] Shiyao Lu,[b] Hu Wu,[b] Xiaohan Cao,[c] Xinghong Zhang[c,] and Shujiang Ding[b,]**

[a] School of Material Science and Chemical Engineering, Harbin University of Science and Technology, Harbin 150080, China.

[b] School of Chemistry, Engineering Research Center of Energy Storage Materials and Chemistry for Universities of Shaanxi Province, State Key Laboratory for Mechanical Behavior of Materials, Xi'an Jiaotong University, Xi'an 710049, China.

[c] National Key Laboratory of Biobased Transportation Fuel Technology, International Research Center for X Polymers, Department of Polymer Science and Engineering, Zhejiang University, Hangzhou 310027, China.

Email: xhzhang@zju.edu.cn; dingsj@mail.xjtu.edu.cn

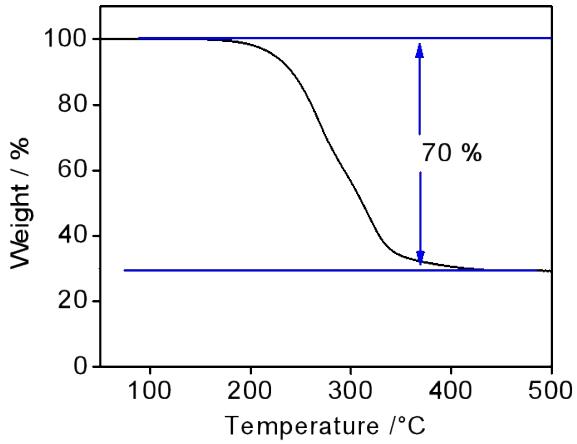

Figure S1. TG plot of the CMK-3/S mixture (30-500 °C) shows the composite's carbon and S content.

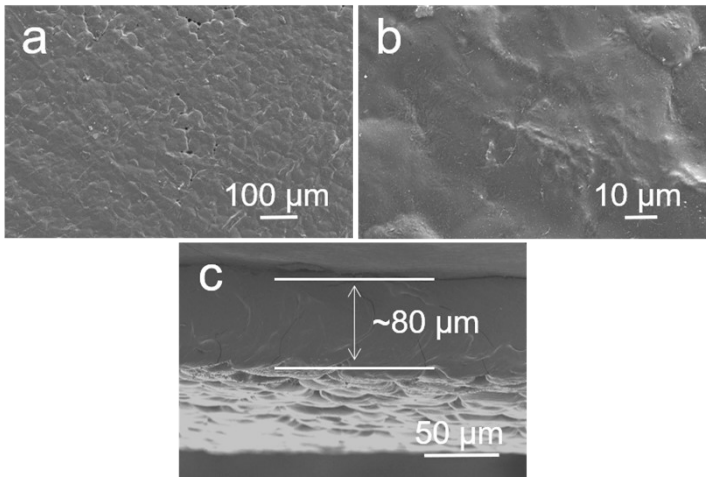

Figure S2. (a) The SEM image of PEO/LiTFSI SPE. The amplified SEM image (b) and the cross-sectional SEM image (c) of PEO/LiTFSI SPE film.

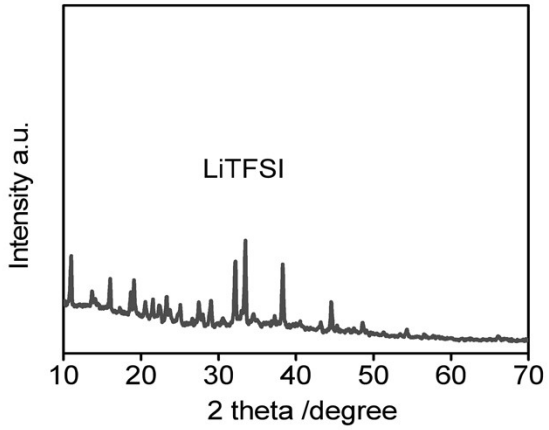

Figure S3. The XRD plot of LiTFSI.

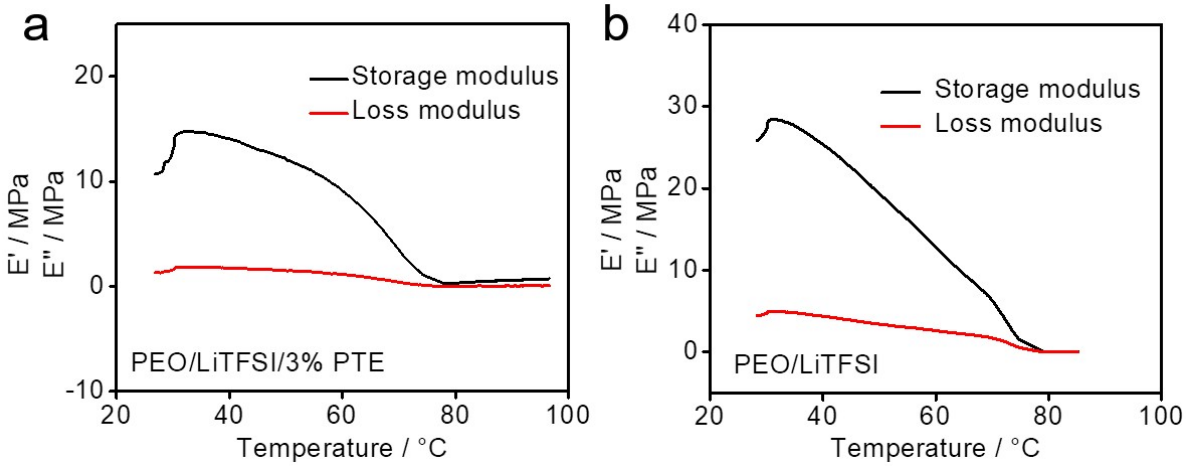

Figure S4. The dynamic mechanical analysis (DMA) of the various solid polymer electrolyte measured in the range 25-100 °C show the plots for elastic modulus and loss modulus of: (a) PEO/LiTFSI/3% PTE CPE, (b) PEO/LiTFSI SPE.

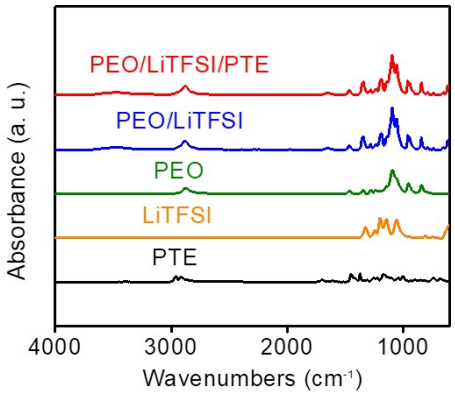

Figure S5. FTIR spectra (600-4000 cm^{-1}) of LiTFSI, PEO, PTE, PEO/LiTFSI and PEO/LiTFSI/PTE CPE.

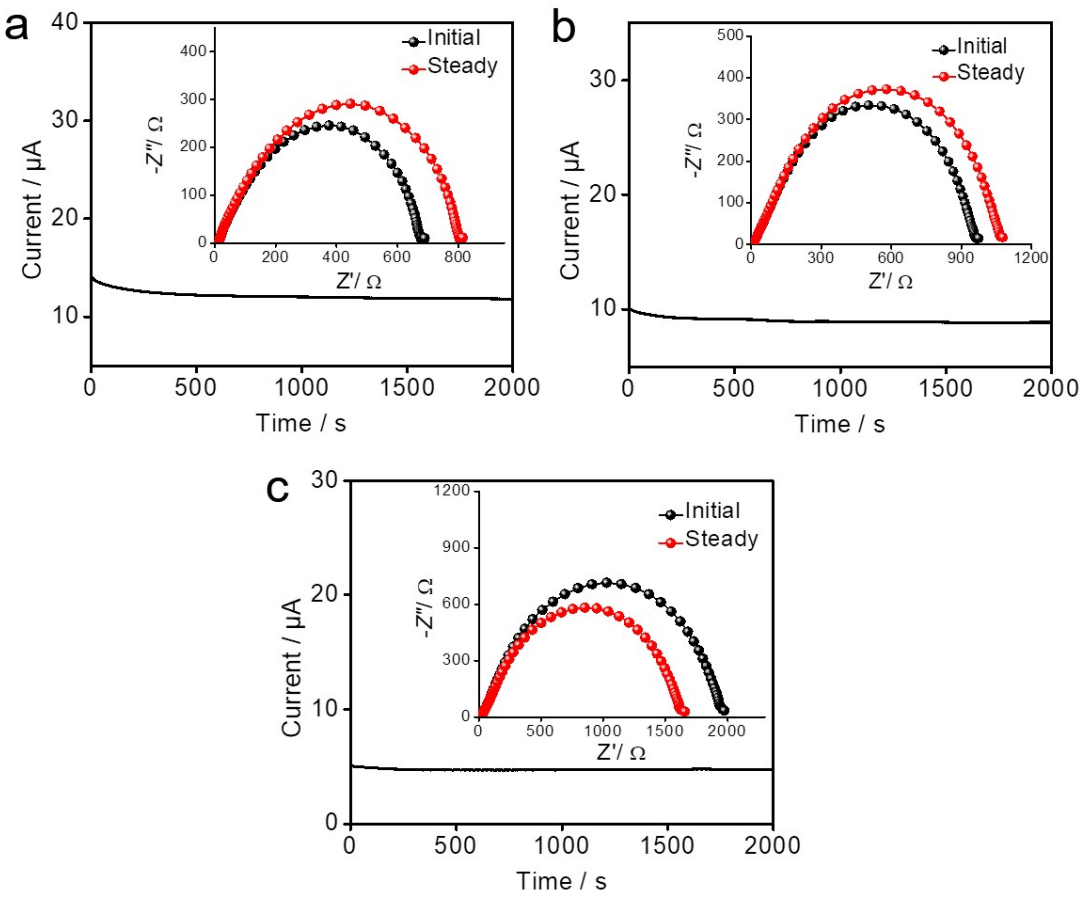

Figure S6. The lithium ion transference number (t_{Li+}) of the composite solid polymer electrolyte with various PTE content: I-t curve and EIS plots before and after polarization for (a) PEO/LiTFSI/1% PTE CPE, (b) PEO/LiTFSI/5% PTE CPE and (c) PEO/LiTFSI/7% PTE CPE.

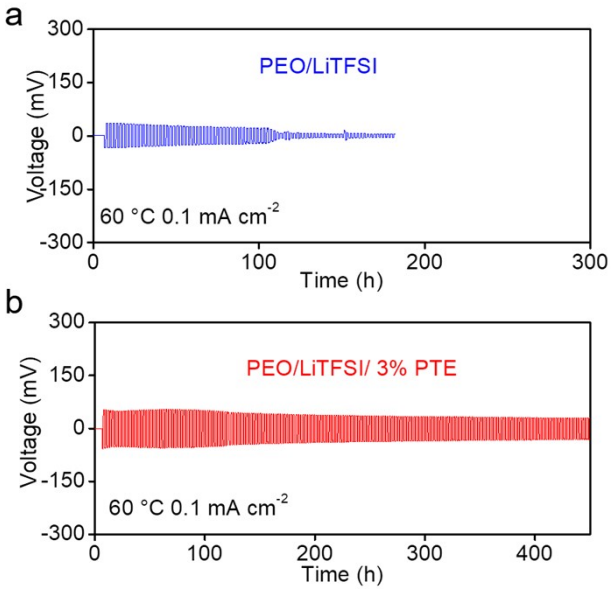

Figure S7. Long-term cycling of symmetrical Li-Li symmetric cells with (a) pure PEO SPE and (b) 3% PTE CPE at 0.1 mA cm^{-2} under 60 °C.

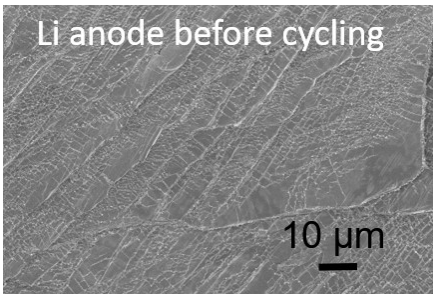

Figure S8. SEM image of the lithium metal anode before cycling.

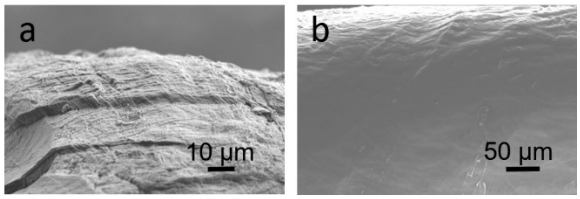

Figure S9. The cross-sectional SEM image of lithium metal anode in the Li-S battery with (a) PEO/LiTFSI SPE and (b) PEO/LiTFSI/PTE CPE after cycling.

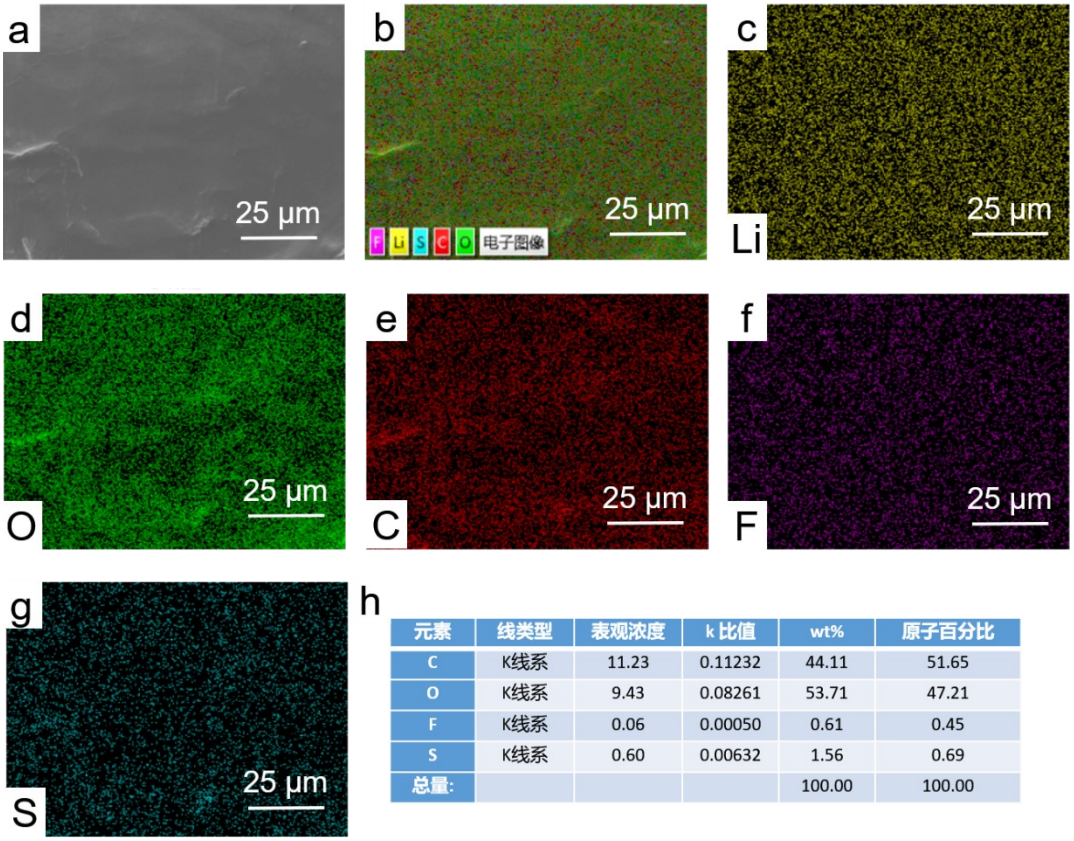

h

元素	线类型	表观浓度	k 比值	wt%	原子百分比
C	K线系	11.23	0.11232	44.11	51.65
O	K线系	9.43	0.08261	53.71	47.21
F	K线系	0.06	0.00050	0.61	0.45
S	K线系	0.60	0.00632	1.56	0.69
总量:				100.00	100.00

Figure S10. (a) The SEM image of the lithium metal anode in the Li-S battery with PEO/LiTFSI/PTE CPE after 10 cycles. (b-g) The EDS mapping of the lithium metal anode in the Li-S battery with PEO/LiTFSI/PTE CPE after 10 cycles. (h) Element content distribution of the lithium metal anode in the Li-S battery with PEO/LiTFSI/PTE CPE after 10 cycles.

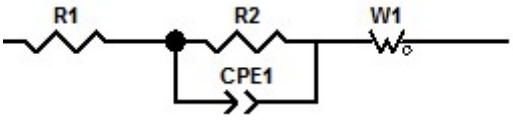

Figure S11. The equivalent circuit diagram of all-solid-state Li-S batteries before and after 5 cycles. R_1, R_2, CPE_1 and W_1 are represented R_0, R_{ct}, CPE and W_0.

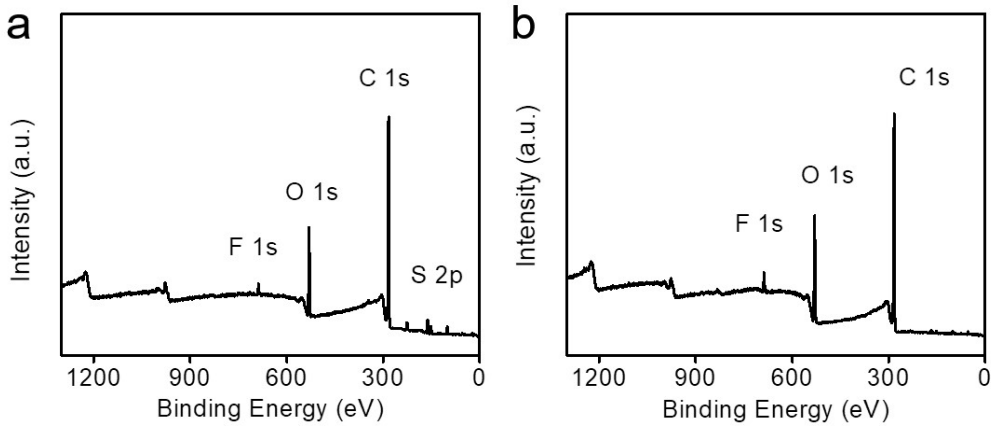

Figure S12. XPS survey scan of the surface for the lithium metal anode after 10 cycles in all-solid-state Li-S batteries with: (a) PEO/LiTFSI/3% PTE CPE and (b) PEO/LiTFSI SPE.

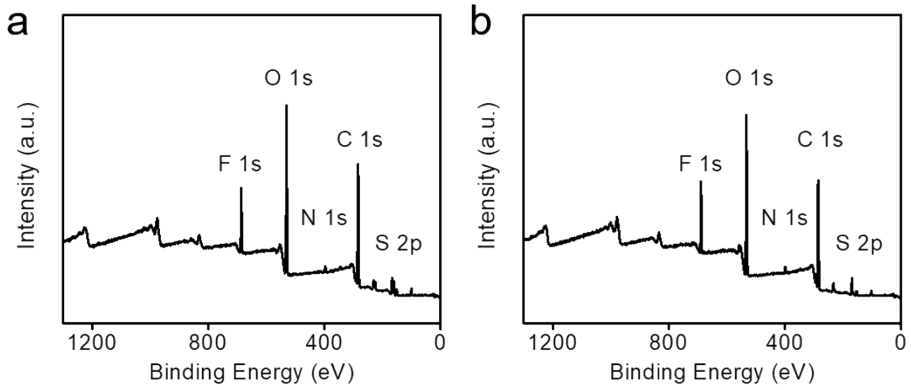

Figure S13. XPS survey scan of the interface between lithium metal anode for PEO/LiTFSI/3% PTE CPE (a) and PEO/LiTFSI SPE (b) in the all-solid-state Li-S battery after 10 cycles.

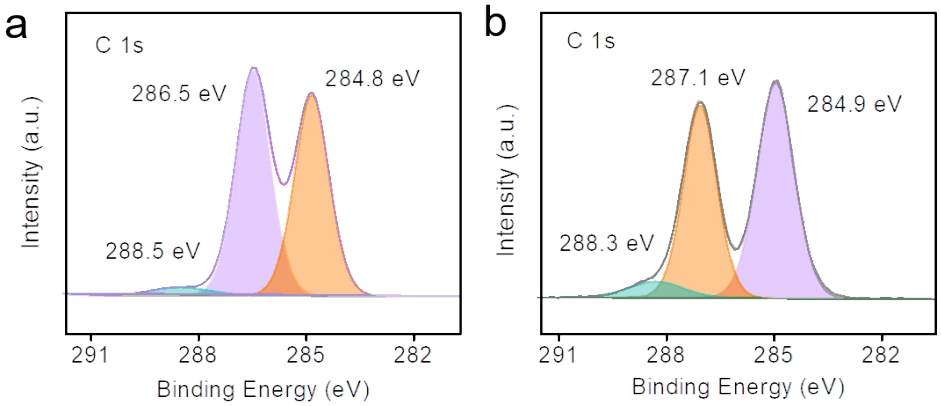

Figure S14. (a) XPS high-resolution C 1s spectra of the surface to the side of lithium metal anode or PEO/LiTFSI/3% PTE CPE in the Li-S battery after 10 cycles. (b) XPS high-resolution C 1s spectra of the surface to the side of lithium metal anode or PEO/LiTFSI SPE in the Li-S battery after 10 cycles.

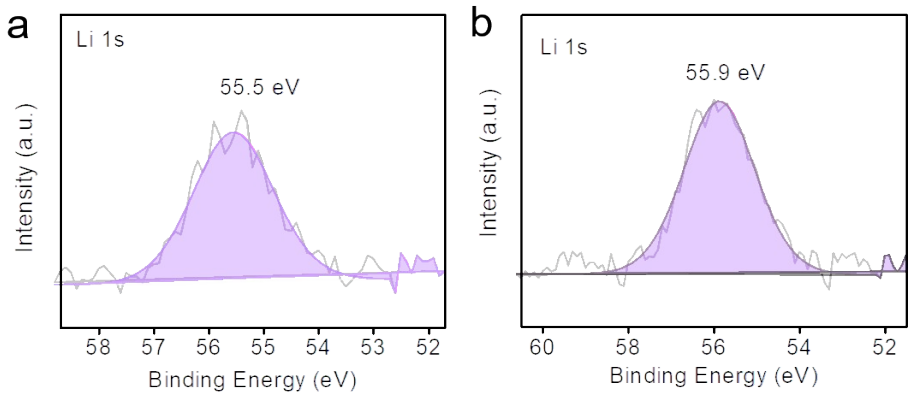

Figure S15. (a) XPS high-resolution Li 1s spectra of the surface for electrolyte to the side of lithium metal anode in the Li-S battery with PEO/LiTFSI/3% PTE CPE after 10 cycles. (b) XPS high-resolution Li 1s spectra of the electrolyte surface to the side of lithium metal anode or PEO/LiTFSI SPE in the Li-S battery after 10 cycles.

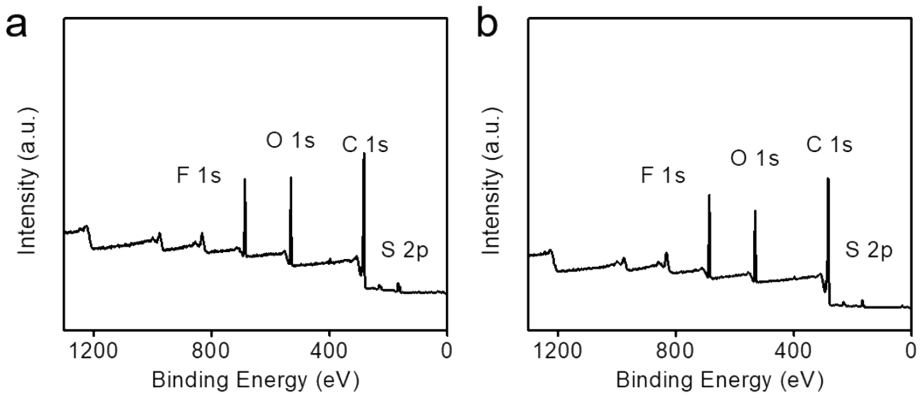

Figure S16. (a) XPS survey scan of the surface to the side of the sulfur cathode in the Li-S battery with PEO/LiTFSI/3% PTE CPE after 10 cycles. (b) XPS survey scan of the surface to the side of the sulfur cathode in the Li-S battery with PEO/LiTFSI SPE after 10 cycles.

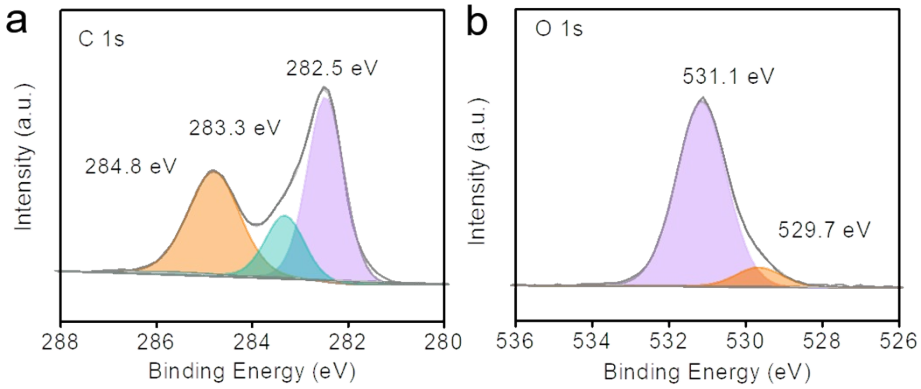

Figure S17. XPS high-resolution C 1s spectra (a) and O 1s spectra (b) of the surface to the side of the sulfur cathode in the Li-S battery with PEO/LiTFSI/3% PTE CPE after 10 cycles.

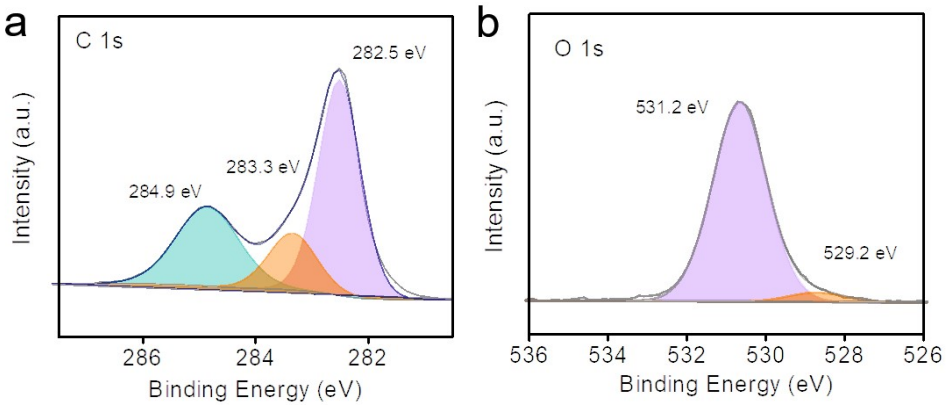

Figure S18. XPS high-resolution C 1s spectra (a) and O 1s spectra (b) of the surface to the side of the sulfur cathode in the Li-S battery with PEO/LiTFSI SPE after 10 cycles.

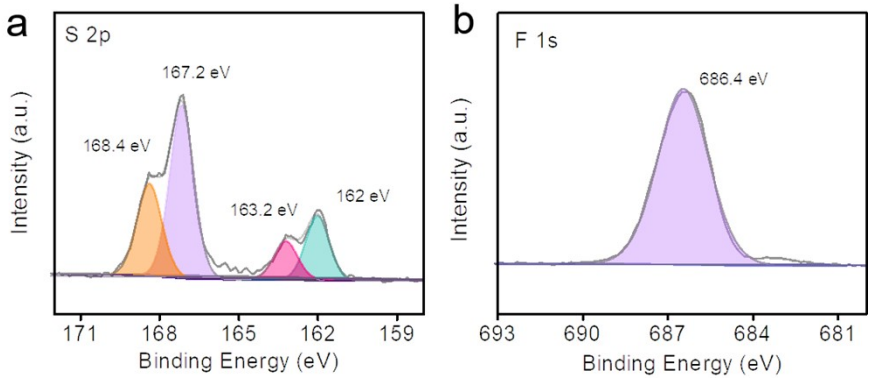

Figure S19. XPS high-resolution S 2p spectra (a) and F 1s spectra (b) of the surface to the side of the sulfur cathode in the Li-S battery with PEO/LiTFSI SPE after 10 cycles.

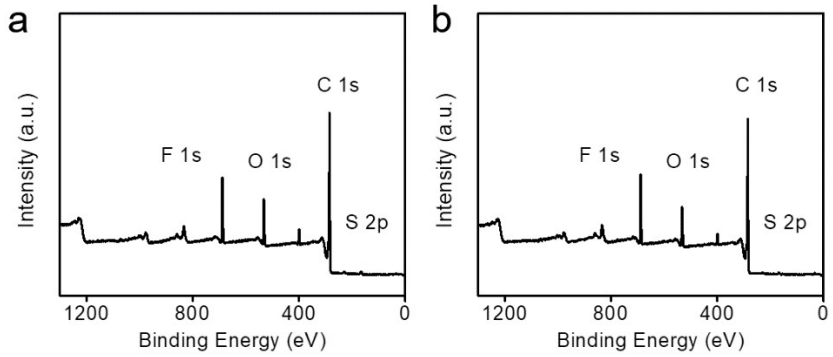

Figure S20. XPS survey scan of the surface of sulfur cathode in the Li-S battery with PEO/LiTFSI/3% PTE CPE (a) and PEO/LiTFSI SPE (b) after 10 cycles.

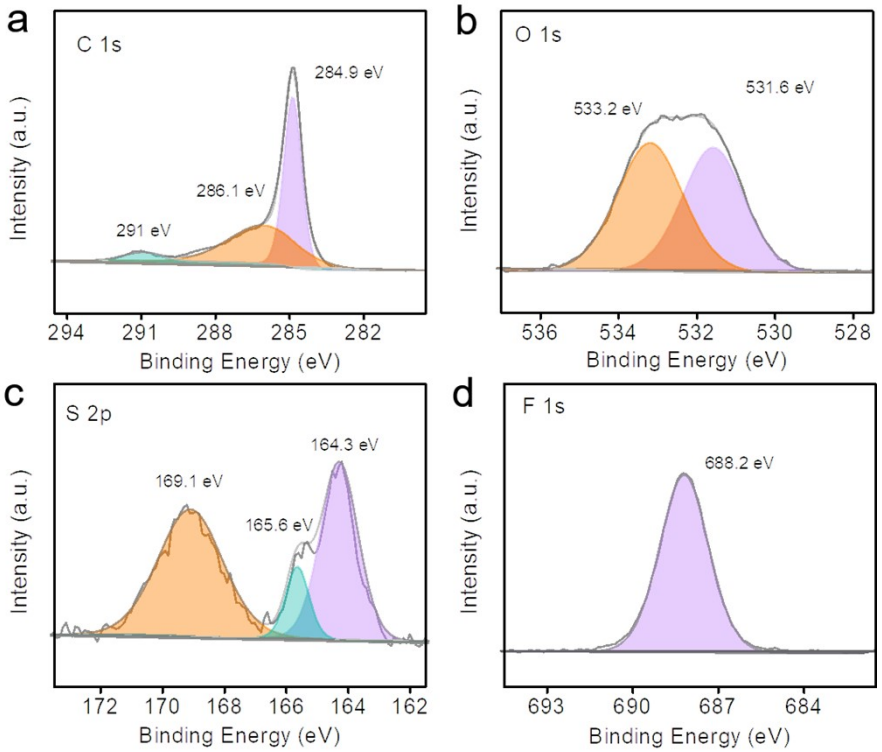

Figure S21. XPS high-resolution C 1s spectra (a), F 1s spectra (b), S 2p (c) and F 1s (d) of the surface of sulfur cathode in the Li-S battery with PEO/LiTFSI/PTE CPE after 10 cycles.

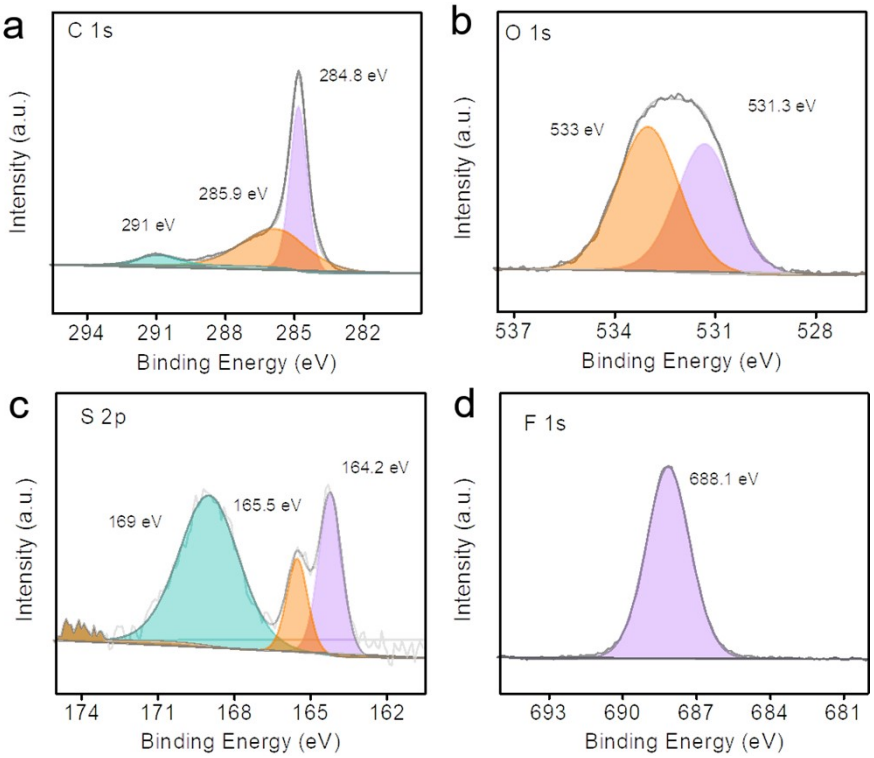

Figure S22. XPS high-resolution C 1s spectra (a), O 1s spectra (b), S 2p spectra (c) and F 1s spectra (d) for the surface of sulfur cathode for PEO/LiTFSI SPE in the battery after 10 cycles.

Table S1. The peaks and corresponding assignments for LiTFSI, PEO, PEO/LiTFSI and PEO/LiTFSI/PTE CPE

Peak assignment	Wavenumber/cm^{-1}			
	PEO	LiTFSI	PEO/LiTFSI	PEO/LiTFSI/PTE
$-CH_2-$ wagging absorptions in trans planar structure	1346.2		1342.1	1342.2
$-CH_2-$ twist in helical structure	1280.6		1280.6	1280.5
$-CH_2-$ twist in trans planar structure	1238.7		1240.7	1240.7
Asymmetric $-SO_2-$ stretching		1325	1333.4	1332.2
Symmetric stretching of $-CF_3$		1244	1231.4	1231.6
Asymmetric stretching of $-CF_3$		1197.7	1189.2	1189.3

Table S2. The corresponding simulated impedance parameters in an equivalent circuit.

	Before cycle		After 5 cycles	
	R_0 (Ω)	R_{ct} (Ω)	R_0 (Ω)	R_{ct} (Ω)
PEO/LiTFSI/3% PTE	14.52	102.4	16.77	123.1

Table S3. Comparison of electrochemical cycle performance of Li/PEO/LiTFSI/PTE CPE/Li with the other reported PEO-based electrolyte.

Electrolyte	Cycle time	Polarization voltage	Current density	Reference
PEO/LiTFSI/PTE CPE	1400 h	~ 25 mV	0.05 mA cm^{-2}	This work
ZnO quantum dots /PEO composite polymer electrolyte	500 h	~ 40 mV	0.1 mA cm^{-2}	Energy Storage Materials, 2021, 43, 258-265.
Al_2O_3 modified PEO-based composite polymer electrolyte	1240 h	~ 40 mV	0.1 mA cm^{-2}	Journal of Electroanalytical Chemistry, 2021, 881, 114916.
SiO_2 based functional polymer electrolyte	1200 h	~ 170 mV	0.1 mA cm^{-2}	Journal of Materials Chemistry A, 2022, 10, 3400-3408.
PVDF/organo-polysulfide polymer electrolyte	250 h	~ 15 mV	0.5 mA cm^{-2}	Journal of Energy Chemistry, 2020, 48, 267-276.
Crosslinked poly(allyl glycidyl ether) polymer electrolyte	255 h	~ 8 mV	0.5 mA cm^{-2}	Electrochimica Acta, 2020, 362, 137141
PVDF/PEO/garnet composite polymer electrolyte	1400 h	~ 80 mV	0.15 mA cm^{-2}	Advanced Energy Materials, 2021, 11, 2101612.
PEO/LLZO NFs-DI-Ca^{2+}/LiTFSI composite polymer electrolyte	1200 h	~ 60 mV	0.1 mA cm^{-2}	ACS Applied Materials & Interfaces, 2022, 14, 5346-5354.
$La_2Zr_2O_7$/PEO solid electrolyte	1600 h	~ 190 mV	0.1 mA cm^{-2}	Energy & Environmental Science, 2022,15, 1503-1511.
PEO/Li_2S_6 composite polymer electrolyte	400 h	25 mV	0.2 mA cm^{-2}	Angewandte Chemie International Edition, 2021, 60, 17701-17706.